Label-free detection of oligonucleotide microarrays by oblique-incidence reflectivity difference method

Xu Wang,[1,2] Kun Yuan,[1] Heng Lu,[1] Juan Wen,[1] Huibin Lu,[1] Kuijuan Jin,[1] Yueliang Zhou,[1] Guozhen Yang,[1,a)] Wei Li,[3] and Kangcheng Ruan[3,a)]
[1]*Beijing National Laboratory for Condensed Matter Physics, Institute of Physics, Chinese Academy of Sciences, Beijing 100190, China*
[2]*Bioinformatics Laboratory and National Laboratory of Biomacromolecules, Institute of Biophysics, Chinese Academy of Sciences, Beijing 100101, China*
[3]*State Key Laboratory of Molecular Biology, Institute of Biochemistry and Cell Biology, Shanghai Institutes for Biological Sciences, Chinese Academy of Sciences, Shanghai 200031, China*

(Received 27 October 2009; accepted 24 January 2010; published online 30 March 2010)

Hybridizations between labeled or label-free targets and corresponding 21-base oligonucleotide probes, concentrations of which range from 0.39 to 50 μM, are detected by oblique-incidence reflectivity difference (OI-RD) method and fluorescence detection. The experimental results demonstrate that the OI-RD method can be utilized to not only distinguish whether the hybridization of oligonucleotides happened but also directly tell the different concentrations of the labeled and unlabeled oligonucleotides on the microarrays. The analysis with a classical three-layer model suggests that single-strand DNA tends to lie on epoxy-functionalized glass slide while the double-strand DNA prefers to have a tilted angle with respect to the slide in our experimental situation. The label-free detection of hybridization of oligonucleotides declares that OI-RD is a promising method for label-free and high-throughput detection of the biological microarrays. © *2010 American Institute of Physics*. [doi:10.1063/1.3327447]

I. INTRODUCTION

The field in biomolecular microarrays and microarray analysis has blossomed immensely since the first paper in 1995.[1] Oligonucleotide microarray, based on specific hybridization between target molecules and corresponding oligonucleotide probes, has become the reference technique to monitor the expression of thousands of genes in a single experiment simultaneously.[2,3] There are many detection schemes for oligonucleotide microarrays based on optical or electrochemical detection.[4,5] Fluorescence detection is the most widely used optical method for its high sensitivity and high throughput.[6] However, the whole procedures including labeling and detecting are very time consuming and costly. Meanwhile, the labeling procedures may often cause some damages to the structure or modifications in the biological activity of the sample.[7,8] For this reason, label-free detection represents an attractive alternative approach for microarray detection. So far, surface plasmon resonance (SPR) is the most widely used technique that has been applied successfully to the detection of label-free biological samples.[9–11] Though SPR has adequate sensitivity to detect low concentrations of biomolecules, the need for high-quality gold film coated on the surface unavoidably increases the difficulty of high throughput detection. Generally, SPR has not been considered to be a high-throughput method yet. Up to now, it is still a big challenge to obtain a label-free and high-throughput detection method for biological microarrays. Landry *et al.*[12] reported the label-free detection of oligonucleotide microarray of 60 nt (nucleotide) probes using *oblique-incidence reflectivity difference* (OI-RD) recently. However, this kind of oligonucleotide microarray is not suitable for the profiling of microRNA (miRNA), a kind of noncoding tiny RNA of about 21 nt in length, which is a rapidly emerging field in life science in recent years.[13,14] In miRNA oligonucleotide microarray, much shorter probes are required due to the small size of miRNA. In this paper, we further detected the synthesized model miRNA with oligonucleotide microarrays of about 30 nt short probes by OI-RD method. The experimental results show that OI-RD can successfully detect oligonucleotide microarray of short probes which is suitable for the miRNA profiling in a label-free and high-throughput manner.

II. EXPERIMENTS

In our early work, OI-RD has been used to *in situ* monitor the growth of oxide films as a particular form of optical ellipsometry.[15,16] The experimental results show that the detection sensitivity for the difference in reflectivity change $\Delta R/R$ between *s*- and *p*-polarized light can reach 2×10^{-5},[17] indicating OI-RD is a high-sensitivity detection technique.

The experimental setup shown in Fig. 1 is similar to those used in film detection, except that the substrate is replaced with a biological microarray lying on a two-dimensional motorized stage. The probe beam from a He–Ne laser is initially *p* polarized. It first passes through a photoelastic modulator (PEM100) that induces the resultant beam to oscillate between *p*- and *s*-polarization with the modulated frequency $\Omega=50$ kHz. An adjustable phase difference between *p*- and *s*-polarized components can be introduced by a phase shifter, typically by rotating the half-wave plate along the optical axis. Subsequently, the laser is focused on the

a)Authors to whom correspondence should be addressed. Electronic addresses: yanggz@aphy.iphy.ac.cn and kcruan@sibs.ac.cn.

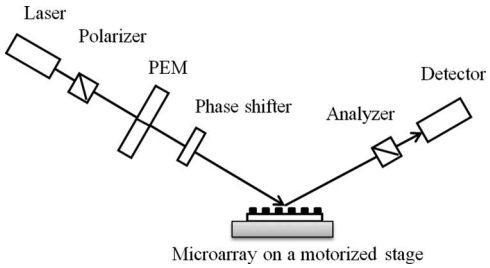

FIG. 1. Sketch of OI-RD system for the detection of oligonucleotide microarrays. The microarray is mounted on a motorized stage that can be driven along *x* and *y* direction, respectively. Laser: He–Ne polarized laser; PEM: Photoelastic modulator.

surface of microarray at an incident angle of 60°. The reflected beam passes through a polarization analyzer and the intensity is detected with a biased silicon photodiode. We monitor the ac component $I(\Omega)$ of the reflected beam intensity at the modulation frequency.

Briefly, let $r_{p0}=|r_{p0}|\exp(i\Phi_{p0})$ and $r_{s0}=|r_{s0}|\exp(i\Phi_{s0})$ denote the respective reflectivity from the functionalized glass surface for *p*- and *s*-polarized light at the wavelength 632.8 nm, and $r_p=|r_p|\exp(i\Phi_p)$ and $r_s=|r_s|\exp(i\Phi_s)$ be the respective reflectivity from oligonucleotide molecules on surface. The changes of reflectivity are defined as $\Delta_p=|(r_p-r_{p0})/r_{p0}|$ and $\Delta_s=|(r_s-r_{s0})/r_{s0}|$. The difference of fractional reflectivity change is Δ_p-Δ_s. In the experiments, we directly measure $I(\Omega)$, which is just proportional to Im$\{\Delta_p$-$\Delta_s\}$. The entire OI-RD detection system was mounted on an optical table and covered by a black box to minimize the effects of stray light, dust, and airflow. The experiments were all performed in an ultraclean room.

We chose a PAGE-purified oligonucleotide as a model miRNA (target), whose sequence (3′ CCT TTA GGG ACC GTT ACA CTA 5′) is consistent with rno-miR-23a. Two different oligonucleotide DNA probes were also designed. 5′-amino-$(A)_{10}$ CTT CAG GTC ATG AGC CTG AT 3′ is designed as a negative control probe and named as Probe-I, which would not hybridize with the model miRNA. 5′-amino-$(A)_{10}$ GGA AAT CCC TGG CAA TGT GAT 3′ is a perfect match to the model miRNA, named as Probe-II. There are 10 deoxyadenosines (Linker) in the 5′ terminus for the probes to minimize the spatial obstacle in hybridization. The model miRNA modified at the 5′ terminus with Cy5 fluorescence label was named as Target-III; the one without fluorescence label was named as Target-IV. In order to detect the specific binding between probes and targets with OI-RD method and fluorescence scanner, and to compare the results from them, different microarrays were designed. First, Probe-I and Probe-II were both printed in triplicate on one slide in a series of concentrations decreasing sequentially by a factor of 2 from 50 to 0.098 μM. The distribution of the spots is shown in Fig. 2(a). The left three columns are Probe-I molecules, and the right three columns are Probe-II molecules. The concentrations are decreasing from top to bottom for every column. The space between probe spots is 400 μm, and the diameter of each spot is about 150 μm. Second, the targets were captured by oligonucleotide probes on the microarray surface in hybridization. In this step, one

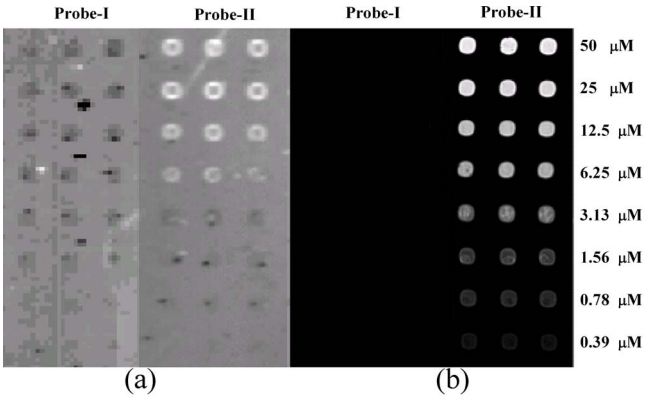

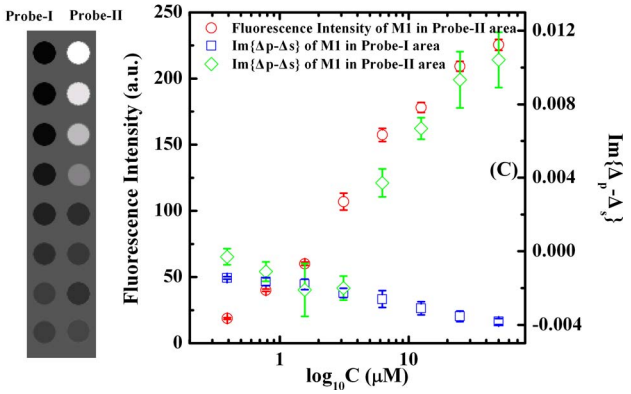

FIG. 2. (Color online) (a) Im$\{\Delta_p$-$\Delta_s\}$ image of labeled microarray M1 after hybridization. (b) Fluorescence image of labeled microarray M1 after hybridization. Probe-I area is in the left, Probe-II area is in the right. (c) Left image: Gray scale image of Im$\{\Delta_p$-$\Delta_s\}$ for Probe-I and Probe-II averaged from each three columns. Right curves: Im$\{\Delta_p$-$\Delta_s\}$ and fluorescence intensities over the printed triplicate spots area vs the concentration.

microarray named as M1 was hybridized with 10 nM Cy5 labeled Target-III at 47 °C (near the melting temperature) overnight. Moreover, in order to try a detection of binding between probes and targets in a label-free fashion by OI-RD, another microarray named as M2 was prepared in a similar way except that the Target-III was replaced by unlabeled Target-IV. The preparation details of oligonucleotide microarrays can be referred to Ref. 3.

III. RESULTS AND DISCUSSION

At first, the microarray M1 was scanned with both fluorescence scanner (LuxScan 10K, CapitalBio Corporation, China) and the OI-RD system to compare the results of specific binding between probes and targets. Figures 2(a) and 2(b) show the Im$\{\Delta_p$-$\Delta_s\}$ and fluorescence images of microarray M1 after hybridization with labeled Target-III, respectively. From Fig. 2(b), we can see that the images of Probe-I area and Probe-II area are different because the Target-III would only hybridize with Probe-II, which reveals the hybridization of the Cy5-labeled Target-III and the complementary Probe-II other than Probe-I. In Fig. 2(a), similarly, the Im$\{\Delta_p$-$\Delta_s\}$ intensities of spots in Probe-II area are also different from those in Probe-I area. What OI-RD detected is consistent with the results from fluorescence image, which well demonstrates that OI-RD method has the

ability to tell whether specific binding occurs. However, the images of Probe-I areas in Figs. 2(a) and 2(b) show that the fluorescence method is incapable of detecting unlabeled molecules mounted on surface. The unhybridized Probe-I molecules (without fluorescence label) can only be detected by OI-RD method.

To make a better contrast, the corresponding quantitative data of OI-RD and fluorescence signals in Figs. 2(a) and 2(b) are presented in Fig. 2(c). We spatially averaged $\mathrm{Im}\{\Delta_p\text{-}\Delta_s\}$ data for Probe-I and Probe-II from each three columns and made an average of them, then we drew a gray scale image in the left side of Fig. 2(c) with the $\mathrm{Im}\{\Delta_p\text{-}\Delta_s\}$ data. The averaged $\mathrm{Im}\{\Delta_p\text{-}\Delta_s\}$ and fluorescence intensity over the printed spot area versus the concentration are also plotted in the right side of Fig. 2(c). The error bars are standard deviations. From Fig. 2(c), we can see that the averaged intensities of $\mathrm{Im}\{\Delta_p\text{-}\Delta_s\}$ and fluorescence have a nearly linear relation in Probe-II area for higher concentrations. For unhybridized Probe-I molecules, the concentrations can also be distinguished by $\mathrm{Im}\{\Delta_p\text{-}\Delta_s\}$.

We now present a quantitative analysis of the OI-RD signals in Fig. 2. Similar to the analysis of OI-RD signals in the oxide film growth,[15] to relate the structural information of a biomolecular layer on a glass slide to the experimentally measured $\Delta_p\text{-}\Delta_s$, we use the Eq. (1) deduced from a classical three-layer model to describe the optical response,[18]

$$\Delta_p\text{-}\Delta_s = -i\left[\frac{4\ \pi\varepsilon_s(\tan\theta_{\mathrm{inc}})^2\cos\theta_{\mathrm{inc}}}{\varepsilon_0^{1/2}(\varepsilon_s-\varepsilon_0)[\varepsilon_s/\varepsilon_0-(\tan\theta_{\mathrm{inc}})^2]}\right] \times \frac{(\varepsilon_d-\varepsilon_s)(\varepsilon_d-\varepsilon_0)}{\varepsilon_d}\left(\frac{d}{\lambda}\right). \quad (1)$$

In this case, θ_{inc} is the incidence angle; ε_0, ε_d, and ε_s are the optical dielectric constants of the ambient, the biomolecular layer and the glass slide, respectively; d is the thickness of biomolecular layer; and λ is the wavelength of incident laser. Noting that the thickness, d, is really its "effective thickness" (d should be replaced by d_{eff}), i.e., average thickness. The effective thickness of oligonucleotides in the microarray M1 before and after hybridization can be determined by Eq. (1). After hybridization, single-strand DNA (ssDNA) oligonucleotides in Probe-II area changed into "linker+double-strand DNA (dsDNA)" while unhybridized ssDNA oligonucleotides in Probe-I area remained to be ssDNAs. The highest concentration 50 μM we used in M1 is near the saturation concentration. It is reported that near the saturation density, the dielectric constant of the ssDNA is expected to be $\varepsilon_{d1}=2.14$, and the dielectric constant of the dsDNA is $\varepsilon_{d2}=2.35$.[19] Using Eq. (1) with $\theta=60°$, $\varepsilon_0=1.0$, and $\varepsilon_s=2.30$ for the glass slide, it is easy to predict that OI-RD signals of oligonucleotide spots should be changed after hybridization. For 50 μM concentration, the $\mathrm{Im}\{\Delta_p\text{-}\Delta_s\}$ intensity before hybridization is -0.004 for ssDNA, we then obtain that the effective thickness of ssDNA $d_{1\mathrm{eff}}$ is about 0.65 nm from Eq. (1). After hybridization, the $\mathrm{Im}\{\Delta_p\text{-}\Delta_s\}$ intensity is 0.01 for dsDNA, which means $d_{2\mathrm{eff}}$ is about 5 nm. It is known that the length for 21 bases is about 7.1 nm. Plus the length of the linker (about 3.4 nm), the whole hybridized DNA should be about 10.5 nm long. The $d_{1\mathrm{eff}}$ is much less than the length of a single stranded oligonucleotide, which means the ssDNAs most lie flat on the glass slide. However, $d_{2\mathrm{eff}}$ is much larger than $d_{1\mathrm{eff}}$, which indicates that the thickness of oligonucleotides after hybridization increases greatly. The increased thickness declares that the oligonucleotides no longer lie flat on the surface since the parts of the oligonucleotides not crosslinked to the glass slide are free to stretch in the direction perpendicular to the glass slide.[20] Meanwhile, $d_{2\mathrm{eff}}$ is only about 5 nm which is still less than the length of a whole hybridized DNA, which suggests that the dsDNA tends to have a tilted angle with respect to the epoxy-functionalized glass.

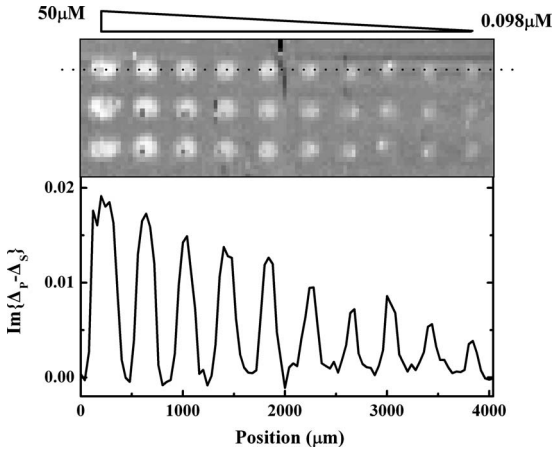

FIG. 3. Top image is the two-dimensional scan image of $\mathrm{Im}\{\Delta_p\text{-}\Delta_s\}$ for unlabeled microarray M2 after hybridization. Bottom curve is the intensity profile taken along the dotted line in the top image.

In addition to the detection of hybridization on microarray M1 between oligonucleotide probes with fluorescence labeled targets, we further detected the hybridization on microarray M2 between oligonucleotide probes with label-free targets using OI-RD, as shown in Fig. 3. The top image in Fig. 3 shows the two-dimensional scan image of $\mathrm{Im}\{\Delta_p\text{-}\Delta_s\}$ for microarray M2 after hybridization. The concentrations of probes from left to right decrease sequentially by a factor of 2 from 50 μM to 0.098 μM. The intensity profile in the bottom of Fig. 3 is taken along the dotted line in the top image of Fig. 3. The result of M2 in Fig. 3 is in accord with that of M1 in Fig. 2, indicating that the OI-RD method can be used to detect not only the hybridization of labeled oligonucleotides but also the hybridization of label-free oligonucleotides. Furthermore, the good intensity profile below Fig. 3(a) demonstrates that we can make OI-RD detection much faster by one-dimensional line scan instead of two-dimensional scan as the spots of the biological sample in the microarray are uniform. It will make the detection of oligonucleotide microarray by OI-RD at least ten times faster. Anyway, the experimental results here have demonstrated that OI-RD method can detect the hybridization of short oligonucleotides in a label-free manner.

Top image in Fig. 4 shows the gray scale image from spatially averaged $\mathrm{Im}\{\Delta_p\text{-}\Delta_s\}$ intensities over every sample area of top image in Fig. 3. It is obvious that the reasonable data treatment makes a better contrast. The bottom of Fig. 4 is the average value of the three rows which also clearly shows a gradual change.

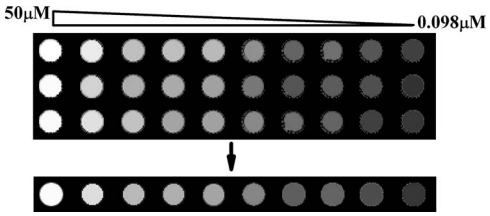

FIG. 4. Gray scale image drew with $\mathrm{Im}\{\Delta_p\text{-}\Delta_s\}$ averaged over every sample area from top image in Fig. 3. The bottom is the further averaged value of the top three rows.

IV. CONCLUSION

In summary, we have successfully detected the model miRNA microarrays by OI-RD method. The experimental results show that the OI-RD method can detect not only the hybridization reactions of short oligonucleotides, but also the different concentrations of labeled and unlabeled oligonucleotide on the microarrays. We can get some structure information about oligonucleotide molecules from the analysis of OI-RD experimental results. It is possible to achieve higher throughput detection of biological microarrays by one-dimensional line scan. The successful detections of short oligonucleotides, similar size of miRNA, demonstrate that the OI-RD is a promising method for label-free and high-throughput detection of the biological microarrays. Further investigations on the detection sensitivity, high-throughput detection and real-time detection in a DNA hybridization reaction are being planned.

ACKNOWLEDGMENTS

The work is supported by The National Basic Research Program in China under Grant No. 2007CB935700.

[1]M. Schena, D. Shalon, R. W. Davis, and P. O. Brown, Science **270**, 467 (1995).
[2]O. Barad, E. Meiri, A. Avniel, R. Aharonov, A. Barzilai, I. Bentwich, U. Einav, S. Glad, P. Hurban, Y. Karov, E. K. Lobenhofer, E. Sharon, Y. M. Shiboleth, M. Shtutman, Z. Bentwich, and P. Einat, Genome Res. **14**, 2486 (2004).
[3]W. Li and K. C. Ruan, Anal. Bioanal. Chem. **394**, 1117 (2009).
[4]Z. S. Wu, J. H. Jiang, L. Fu, G. L. Shen, and R. Q. Yu, Anal. Biochem. **353**, 22 (2006).
[5]J. Wang, G. D. Liu, and A. Merkoci, J. Am. Chem. Soc. **125**, 3214 (2003).
[6]A. P. Abel, M. G. Weller, G. L. Duveneck, M. Ehrat, and H. M. Widmer, Anal. Chem. **68**, 2905 (1996).
[7]A. Eing and M. Vaupel, *Imaging Ellipsometry in Biotechnology*, 2nd ed. (Verlag Axel Gierspeck, Göttingen, 2002), pp. 1–10.
[8]X. D. Zhu, J. P. Landry, Y. S. Sun, J. P. Gregg, K. S. Lam, and X. W. Guo, Appl. Opt. **46**, 1890 (2007).
[9]B. P. Nelson, A. G. Frutos, J. M. Brockman, and R. M. Corn, Anal. Chem. **71**, 3928 (1999).
[10]L. S. Jung, C. T. Campbell, T. M. Chinowsky, M. N. Mar, and S. S. Yee, Langmuir **14**, 5636 (1998).
[11]F. Mannelli, A. Minunni, S. Tombelli, R. H. Wang, M. M. Spiriti, and M. Mascini, Bioelectrochemistry **66**, 129 (2005).
[12]J. P. Landry, X. D. Zhu, and J. P. Gregg, Opt. Lett. **29**, 581 (2004).
[13]R. Q. Liang, W. Li, Y. Li, C. Y. Tan, J. X. Li, Y. X. Jin, and K. C. Ruan, Nucleic Acids Res. **33**, e17 (2005).
[14]M. D. Kane, T. A. Jatkoe, C. R. Stumpf, J. Lu, J. D. Thomas, and S. J. Madore, Nucleic Acids Res. **28**, 4552 (2000).
[15]X. Wang, K. J. Jin, H. B. Lu, Y. Y. Fei, X. D. Zhu, and G. Z. Yang, J. Appl. Phys. **102**, 053107 (2007).
[16]X. Wang, Y. Y. Fei, H. B. Lu, K. J. Jin, X. D. Zhu, Z. H. Chen, and G. Z. Yang, J. Phys.: Condens. Matter **19**, 026206 (2007).
[17]X. D. Zhu, H. B. Lu, G. Z. Yang, Z. Y. Li, B. Y. Gu, and D. Z. Zhang, Phys. Rev. B **57**, 2514 (1998).
[18]X. D. Zhu, Y. Y. Fei, X. Wang, H. B. Lu, and G. Z. Yang, Phys. Rev. B **75**, 245434 (2007).
[19]S. Elhadj, G. Singh, and R. F. Saraf, Langmuir **20**, 5539 (2004).
[20]J. P. Landry, X. D. Zhu, J. P. Gregg, and X. W. Guo, Proc. SPIE **5328**, 121 (2004).